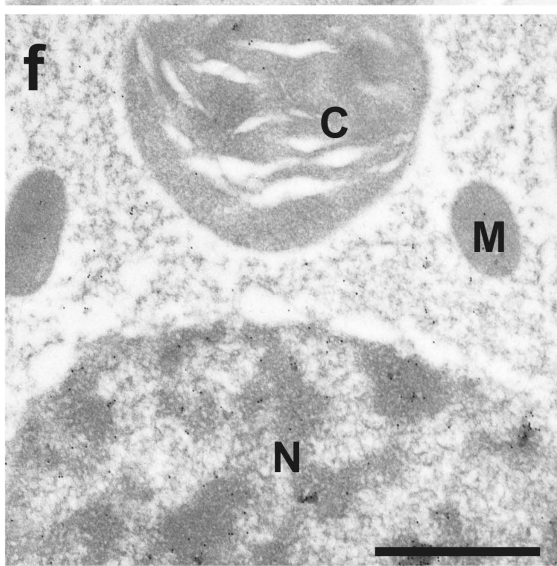
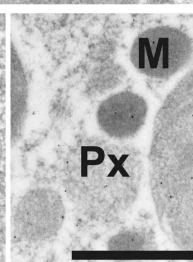
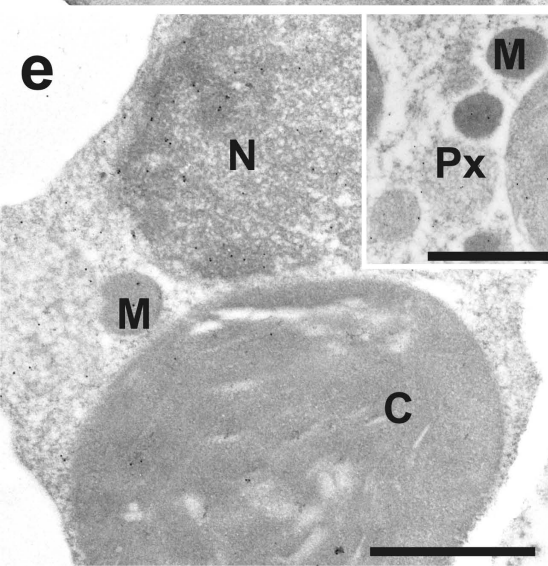
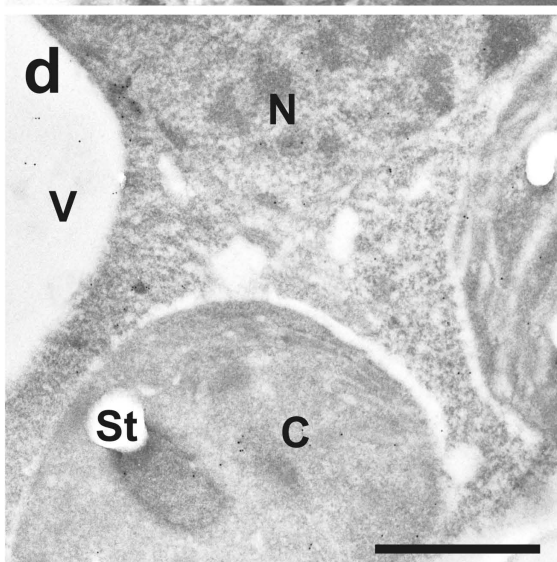
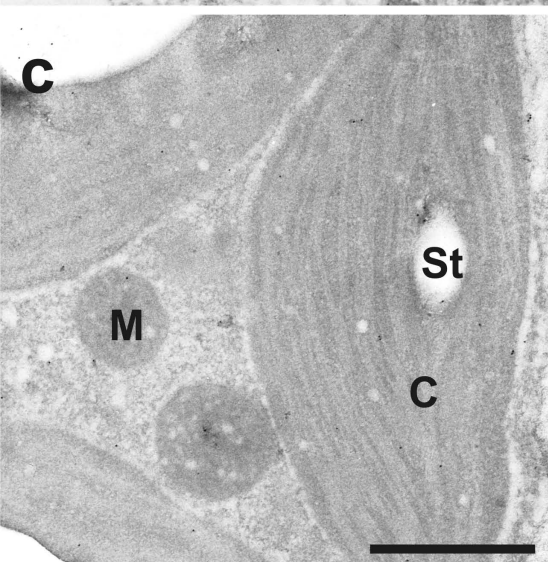
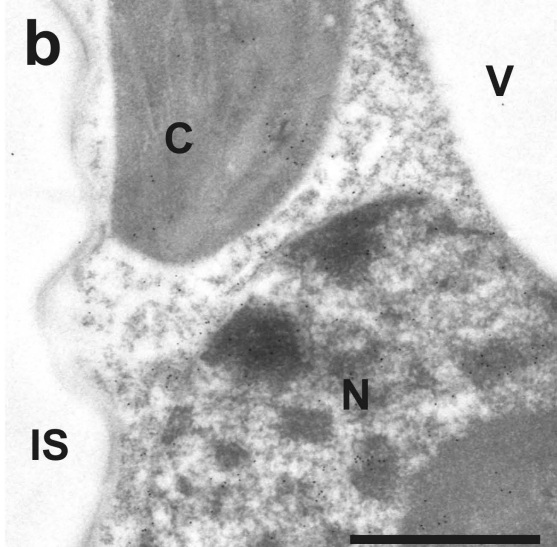
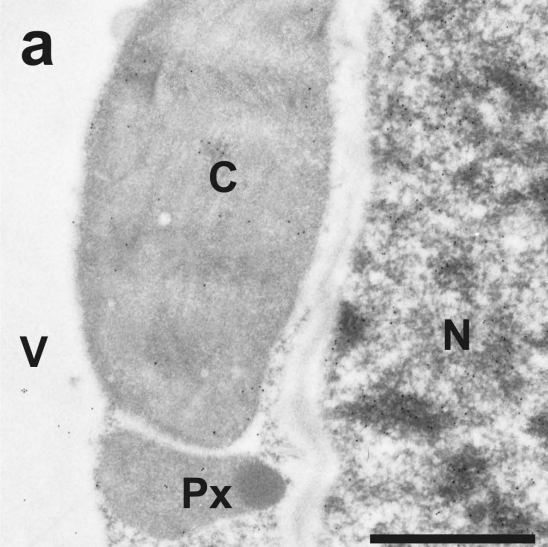
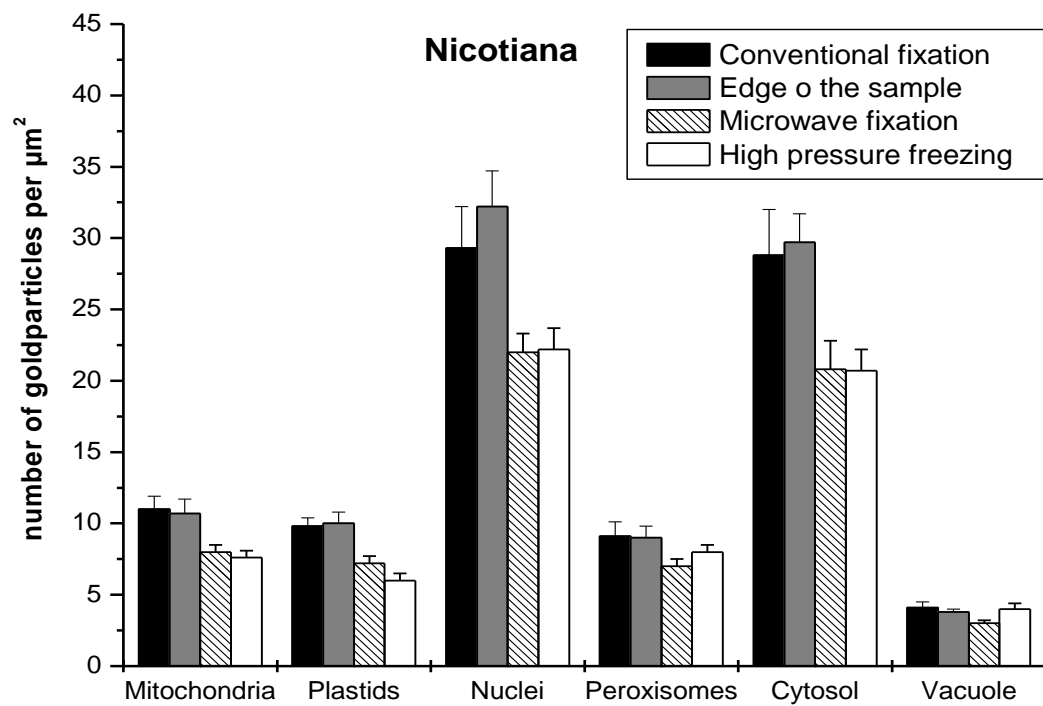
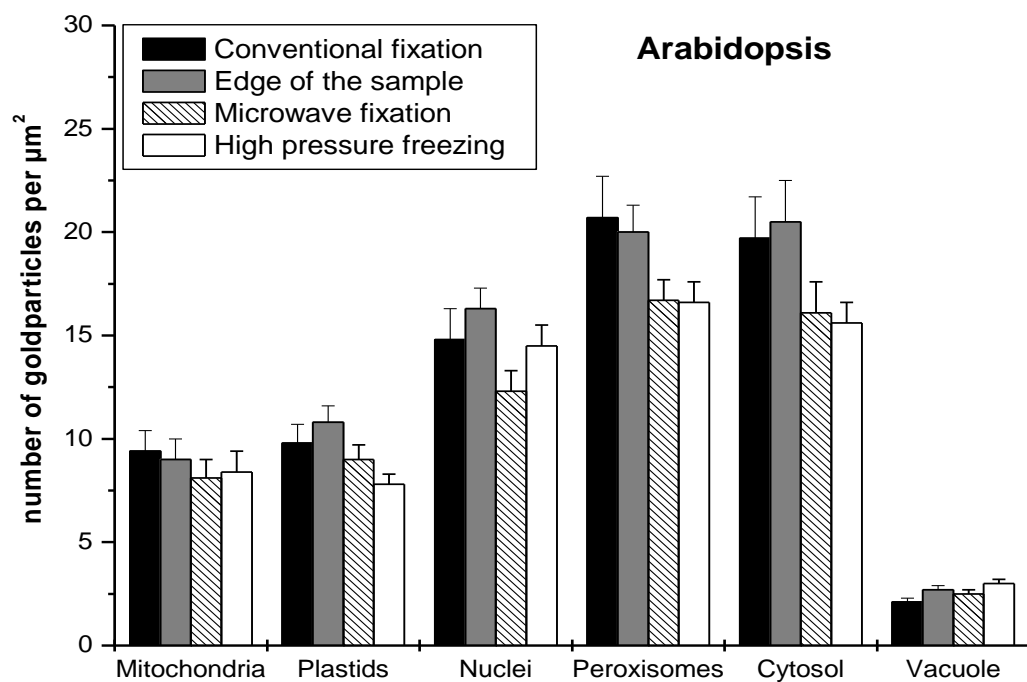


Supplemental Fig. S1 Transmission electron micrographs of the subcellular distribution of ascorbate in *Arabidopsis thaliana* Col-0 plants (a, c, e) and *Nicotiana tabacum* (b, d, f) plants after conventional fixation at the edge of the sample (a, b), microwave fixation (c, d) and high pressure freezing and freeze substitution (e, f). Gold particles bound to ascorbate could be found in different densities within chloroplast (C), mitochondria (M), nuclei (N), peroxisomes (Px), vacuoles (V) and the cytosol but not in cell walls (CW) and intercellular spaces (IS). Bars=1 $\mu$ m (TIFF 9990 kb)

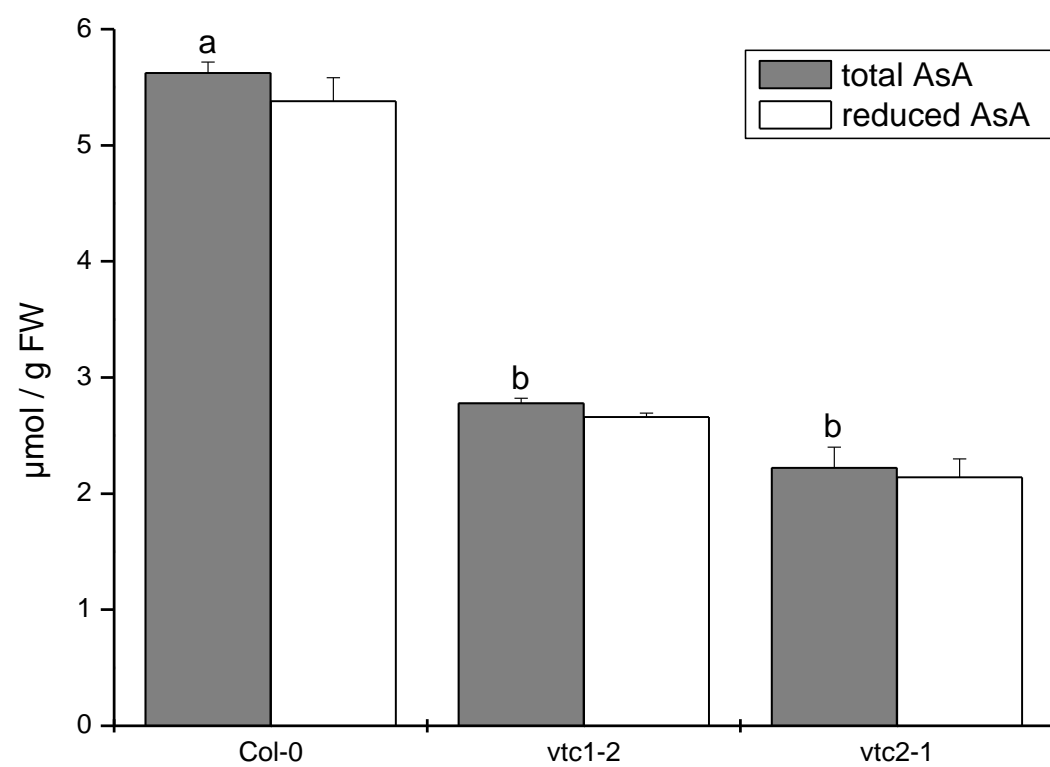
Supplemental Fig. S2 Quantitative analysis of compartment specific ascorbate labeling in *Arabidopsis* and *N. tabacum* leaves after different types of sample preparation. Values are means with standard errors and document the amount of gold particles per  $\mu$ m<sup>2</sup>. n > 20 for peroxisomes and vacuoles and n > 60 for all other cell structures (DOC 224 kb)

Supplemental Fig. S3 Biochemical measurement of total and reduced ascorbate (AsA) contents in *Arabidopsis* plants. Values are means with standard deviations. Significant differences between the samples are indicated by different lower case letters; samples which are significantly different from each other have no letter in common. P<0.05 was regarded significant analyzed by the Kruskal-Wallis test, followed by post hoc comparison according to Conover. n =6 samples (DOC 80 kb)





Supplemental Figure 2



Supplemental Figure 3